

# Solubility and Micellization Behavior of C<sub>60</sub> Fullerenes with Two Well-Defined Polymer Arms

Haruyuki Okamura, Nobuhiro Ide, Masahiko Minoda, Koichi Komatsu, and Takeshi Fukuda\*

*Institute for Chemical Research, Kyoto University, Uji, Kyoto 611, Japan*

*Received November 17, 1997; Revised Manuscript Received January 12, 1998*

**ABSTRACT:** 1,4-Disubstituted, low-polydispersity C<sub>60</sub> derivatives of the types C<sub>60</sub>–(PS)<sub>2</sub>, C<sub>60</sub>–(PVP)<sub>2</sub>, and C<sub>60</sub>–(PS–PVP)<sub>2</sub>, where PS is polystyrene, PVP is poly(*p*-vinylphenol), and PS–PVP is a diblock copolymer of this sequence, were prepared by applying the nitroxide-controlled free radical polymerization technique and studied with their solubility behaviors in some organic solvents. The first clear experimental evidence was obtained for the formation of multimolecular micelles of C<sub>60</sub>-bearing polymers under certain conditions: for example, light-scattering measurements showed that the C<sub>60</sub>–(PVP)<sub>2</sub>, C<sub>60</sub>–(PS–PVP)<sub>2</sub>, and C<sub>60</sub>–(PS)<sub>2</sub> samples with a number-average molecular weight of a polymer arm roughly about 10 000 formed stable micelles in dilute tetrahydrofuran (THF) solution with association numbers of about 20, 6, and 1 (no micellization), respectively. The solvent power of THF for the mother polymers increases in this order. The saturation solubilities *S*<sub>C<sub>60</sub></sub> of the C<sub>60</sub> moiety in C<sub>60</sub>–(PS)<sub>2</sub> and C<sub>60</sub>–(PVP)<sub>2</sub> were determined as a function of the PS and PVP chain lengths, showing that, in THF, the *S*<sub>C<sub>60</sub></sub> in the PS adduct is exceptionally large, much larger than that in the PVP adduct of the same chain length, in accord with the mentioned micellization tendency in dilute solution. On the other hand, C<sub>60</sub>–(PVP)<sub>2</sub> showed a reasonable solubility in a polar solvent (methanol), in which C<sub>60</sub>–(PS)<sub>2</sub> was little soluble. The micellization was found to be accompanied by characteristic changes in the UV–vis spectra, depending on micelle size.

## Introduction

Fullerene has attracted much attention due to its unique chemical and physical properties.<sup>1</sup> Unfortunately, the ability to fabricate fullerene-based devices has been limited due to its poor solubility and processability. Polymer-bound fullerenes are particularly interesting because they can have the high solubility and processability of polymers as well as the unique properties of fullerene. Hence various kinds of C<sub>60</sub>-containing polymers have been synthesized and studied with their optical, electrical, and solubility properties.<sup>2–6</sup> However, the information provided by these studies has often been limited.

As indicated above, C<sub>60</sub> has very limited solubilities in solvents: no solvent is known that is miscible with C<sub>60</sub> in all proportions. The maximum saturation solubility has been obtained with 1-chloronaphthalene at 51 mg/mL.<sup>7</sup> Although C<sub>60</sub> has virtually no solubility in water, it can be solubilized in surfactant solutions via incorporation into the hydrophobic core.<sup>8</sup> Interestingly, the formation of colloidal forms of C<sub>60</sub> in aqueous surfactant solutions drastically changes the UV–vis spectrum from that in a molecularly dispersed state.<sup>8a</sup> Another useful method to solubilize C<sub>60</sub> is derivatization. The solubility of a C<sub>60</sub>-containing polymer is, in a high-molecular weight limit of the polymer, expected to be essentially the same as that of the mother polymer, as in fact reported.<sup>4d</sup> However, the concentration of the C<sub>60</sub> moiety itself in such a limit is small because of the small fraction of C<sub>60</sub> in the polymer. The maximum saturation solubility of the C<sub>60</sub> moiety in a solvent will be obtained when the C<sub>60</sub> fraction in the polymer and the solubility of the mother polymer are optimized. Thus, the discussion of C<sub>60</sub> solubility by derivatization requires us to study the solubility of the derivatives as a function of the chain length of the polymer moiety as

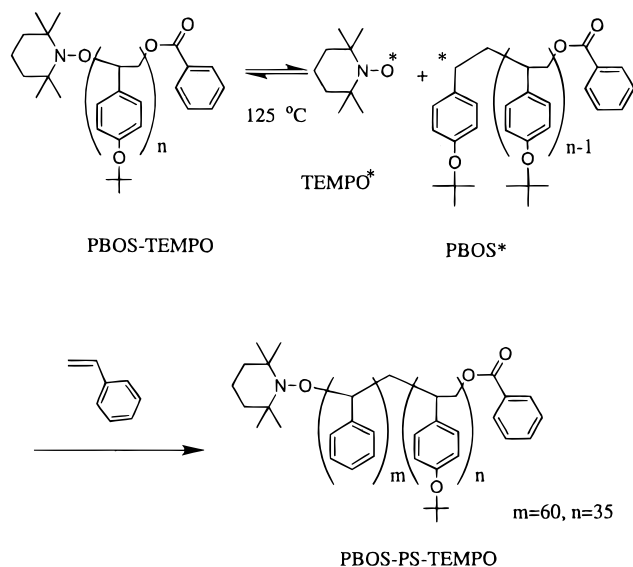
well as the solubility of the mother polymer itself. Such a systematic study has never been reported before this work. Here we have prepared 1,4-disubstituted, low-polydispersity C<sub>60</sub> derivatives of the types C<sub>60</sub>–(PS)<sub>2</sub>, C<sub>60</sub>–(PVP)<sub>2</sub>, and C<sub>60</sub>–(PS–PVP)<sub>2</sub> by applying the nitroxide-controlled free radical polymerization technique,<sup>9</sup> where PS, PVP, and PS–PVP denote polystyrene, poly(*p*-vinylphenol),<sup>10</sup> and PS–PVP type diblock copolymer,<sup>10</sup> respectively. This synthetic procedure was previously shown to be a simple and versatile one to yield well-defined C<sub>60</sub> 1,4-bisadducts.<sup>5</sup>

Another important problem addressed in this work is the states of solution, i.e., monomolecularly dispersed versus multimolecularly associated state of the C<sub>60</sub>–polymers in solution. The first direct experimental evidence will be presented showing that the C<sub>60</sub>–polymers form multimolecular micelles depending on the solubility and length of the polymer moiety and that the micellization accompanies characteristic changes in the UV–vis spectra, similar to those observed for pure C<sub>60</sub> in aqueous surfactant solutions.<sup>8a</sup>

## Experimental Section

**Measurements.** NMR spectra were observed at 270 MHz for <sup>1</sup>H and 100 MHz for <sup>13</sup>C NMR. UV–vis spectra were taken on a Shimadzu UV-2100. Static light-scattering measurements were made in tetrahydrofuran (THF) solvent at 25 °C by a DLS-7000 photometer (Otsuka Electronics, Japan), which was calibrated with benzene. The refractive index increment (*dn/dc*) in THF solution at 25 °C was measured by a DRM1030 differential refractometer (Otsuka Electronics). Gel permeation chromatography (GPC) was carried out in THF on a Tosoh HLC-802UR chromatograph (Tokyo, Japan) equipped with polystyrene gel columns (G2500H6 + G3000H6 + G4000H6; exclusion limit = 1.0 × 10<sup>6</sup>; 8.0 mm i.d. × 60 cm) and refractive index/ultraviolet dual-mode detectors. The system was calibrated with Tosoh standard PSs.

Scheme 1



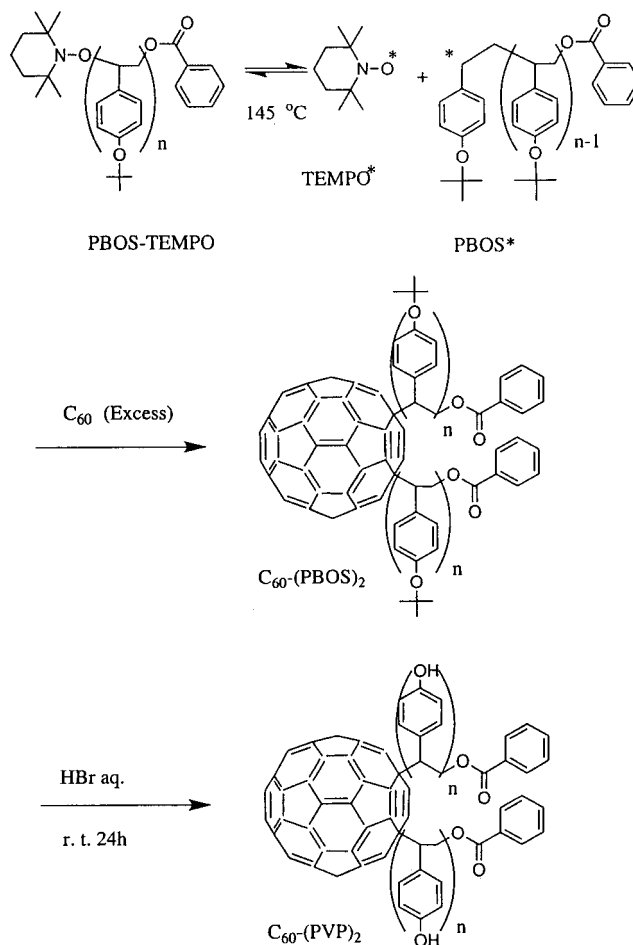
**Materials.**  $C_{60}$ , THF, *o*-dichlorobenzene (ODCB), benzoyl peroxide (BPO; Nacalai Tesque, Japan), and styrene were purified as described previously.<sup>2</sup> *p*-*tert*-Butoxystyrene, kindly donated by Hokko Chemicals (Japan), was washed three times with 10 wt % aqueous NaOH solution and three times with distilled water and dried over anhydrous sodium sulfate. The filtered dry monomer was stored at  $-15\text{ }^{\circ}\text{C}$  in an ampule.<sup>10</sup> TEMPO (Aldrich) was used as received. Deionized water was distilled before use.

**Preparation of PS-TEMPO and PBOS-TEMPO.** The polystyryl adduct with TEMPO (PS-TEMPO) was prepared as described previously.<sup>2,9d</sup> In a typical run to prepare a PBOS adduct with TEMPO,<sup>10</sup> a mixture of BOS, BPO ( $1.02 \times 10^{-1}\text{ mol L}^{-1}$ ), and TEMPO ( $1.05 \times 10^{-1}\text{ mol L}^{-1}$ ) was charged in a glass tube, degassed with several freeze-thaw cycles, and sealed off under vacuum. Then, the mixture was heated at  $95\text{ }^{\circ}\text{C}$  for 3.5 h and at  $125\text{ }^{\circ}\text{C}$  for 3 h to yield a polymer. The polymer was recovered as a precipitate from a large excess of methanol, purified by reprecipitation with a chloroform (solvent)/methanol (nonsolvent) system, and thoroughly dried (conversion: 50.5%), which, according to the PS-calibrated GPC, had a number-average molecular weight  $M_n$  of 2600 and a  $M_w/M_n$  ratio of 1.12, where  $M_w$  is the weight-average molecular weight.

**Preparation of PBOS-PS-TEMPO (Scheme 1).** A PBOS-TEMPO adduct (0.30 g,  $M_n = 6100$ ,  $M_w/M_n = 1.08$ ), obtained as above, was dissolved in styrene (0.92 mL) and heated at  $125\text{ }^{\circ}\text{C}$  for 2 h to obtain a PBOS-PS type block copolymer end-capped by TEMPO (PBOS-PS-TEMPO: 0.45 g,  $M_n = 13500$ ,  $M_w/M_n = 1.15$ ).

**Preparation and Purification of  $C_{60}$ -(PS)<sub>2</sub>,  $C_{60}$ -(PBOS)<sub>2</sub>, and  $C_{60}$ -(PS-PBOS)<sub>2</sub>.** Preparation and purification of  $C_{60}$ -(PS)<sub>2</sub>,  $C_{60}$ -(PBOS)<sub>2</sub>, and  $C_{60}$ -(PS-PBOS)<sub>2</sub> were carried out as described previously.<sup>2</sup> For example, PS-TEMPO ( $6.90 \times 10^{-4}\text{ mol L}^{-1}$ ) and  $C_{60}$  ( $2.78 \times 10^{-3}\text{ mol L}^{-1}$ ) were dissolved in ODCB (5.00 mL), charged in a glass tube, degassed with several freeze-thaw cycles, and sealed off under vacuum. Then, the mixture was heated at  $145\text{ }^{\circ}\text{C}$  for 24 h. The product was a mixture of  $C_{60}$ -PS adducts, unreacted PS, and unreacted  $C_{60}$ . Since the solubility of  $C_{60}$  in THF is very low, virtually all (unreacted)  $C_{60}$  was removed as a precipitate by pouring the reaction mixture into THF (50 mL). The supernatant was dried by evaporation, to which 5.0 mL of benzene was added to dissolve the polymer. To this solution was slowly added 5.0 mL of methanol, and the precipitate was recovered by decantation. Since  $C_{60}$ -PS adducts and PS (or PS-TEMPO) have largely different solubilities in organic solvents, this process was effective enough to separate  $C_{60}$ -PS (precipitate) from PS (in solution). In fact, it was confirmed that the supernatant contained no  $C_{60}$  derivatives and that

Scheme 2



the PS-TEMPO adduct was perfectly soluble in the benzene/methanol mixture. All precipitate was carefully collected by centrifugation. The decanted solution was confirmed to contain only unreacted PS by  $^1\text{H}$  NMR, UV, and GPC.  $C_{60}$ -(PBOS)<sub>2</sub> and  $C_{60}$ -(PS-PBOS)<sub>2</sub> were prepared and purified similarly.

**Hydrolysis of PBOS Moieties (Scheme 2).** Hydrolysis of PBOS and PBOS segments were carried out as described previously.<sup>10,11</sup> For example, 1 g of PBOS was dissolved in 1,4-dioxane (20 mL), and hydrobromic acid (8.6 N, 1.3 mL) was added. The solution was then stirred magnetically at room temperature for 24 h and poured into water (200 mL). The precipitate was filtered off, again dissolved in 1,4-dioxane (15 mL), precipitated in hexane (180 mL), recovered by filtration, and finally freeze-dried twice from 1,4-dioxane to give poly(*p*-vinylphenol) (PVP) as a white powder with a quantitative yield.

**Saturation Solubilities of  $C_{60}$ -(PS)<sub>2</sub> and  $C_{60}$ -(PVP)<sub>2</sub>.** All operations were conducted in an air-conditioned room kept at  $25\text{ }^{\circ}\text{C}$ . A 40 mg quantity of each polymer sample was mixed with 0.1 mL of a test solvent in a centrifuge tube. After 1 min of sonication, the mixture was centrifuged for 20 min. The supernatant (10  $\mu\text{L}$ , measured by microsyringe) was diluted to 100 or 500 times by the test solvent, and the concentration of the  $C_{60}$  moiety was determined by measuring the UV-vis absorption intensity at 440 nm and using the known molar absorption coefficient of  $C_{60}$ -(BS)<sub>2</sub> at 440 nm.<sup>5</sup>

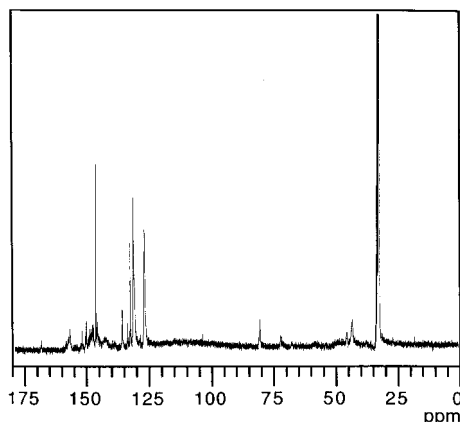
## Results and Discussion

**Synthesis and Characterization of  $C_{60}$ -(PBOS)<sub>2</sub> and  $C_{60}$ -(PS-PBOS)<sub>2</sub>.** From a synthetic viewpoint, this work is a simple extension of the previous one<sup>5</sup> in which well-defined 1,4-bisadducts of  $C_{60}$  with PSs were prepared by the reaction of PS-TEMPO adducts with

**Table 1.** Reaction of TEMPO Adducts with C<sub>60</sub><sup>a</sup>

| precursor (TEMPO adduct)     |   | product (C <sub>60</sub> adduct) |   |  |  |
|------------------------------|---|----------------------------------|---|--|--|
| code                         | <i>M<sub>n</sub></i> ( <i>M<sub>w</sub></i> / <i>M<sub>n</sub></i> )<br>by GPC <sup>b</sup> | yield <sup>c</sup><br>(%)        | <i>M<sub>n</sub></i> ( <i>M<sub>w</sub></i> / <i>M<sub>n</sub></i> )<br>by GPC <sup>b</sup> | <i>M<sub>n</sub></i><br>by UV <sup>d</sup> | <i>M<sub>n</sub></i><br>calcd <sup>e</sup> |
| PBOS-TEMPO-1                 | 890 (1.16)  | 31                               | 1320 (1.31)   | 1800                                       | 2300                                       |
| PBOS-TEMPO-2                 | 2600 (1.12)   | 44                               | 4200 (1.27)   | 4600                                       | 5700                                       |
| PBOS-TEMPO-3                 | 5200 (1.13)   | 52                               | 9300 (1.21)   | 10200                                      | 10900                                      |
| PBOS-TEMPO-4                 | 9800 (1.14)   | 42                               | 17300 (1.24)  | 18800                                      | 20100                                      |
| PBOS-PS-TEMPO-5 <sup>f</sup> | 13500 (1.15)  | 46                               | 24600 (1.27)  | 26100                                      | 27500                                      |

<sup>a</sup> In *o*-dichlorobenzene (145 °C, 24 h); [TEMPO adduct] =  $3.5 \times 10^{-5}$  mol L<sup>-1</sup> and [C<sub>60</sub>] =  $1.4 \times 10^{-4}$  mol L<sup>-1</sup> in all cases. <sup>b</sup> Calibrated by standard PSs. <sup>c</sup> 100(wt of PBOS in C<sub>60</sub>-PBOS)/(wt of PBOS-TEMPO). <sup>d</sup> Calculated on the basis of the molar absorption coefficient of C<sub>60</sub>-(BS)<sub>2</sub> of  $5.01 \times 10^3$  mol<sup>-1</sup> mL cm<sup>-1</sup> (440 nm). <sup>e</sup> Calculated for bisadduct structure. <sup>f</sup> *M<sub>n</sub>*<sub>PBOS</sub>/*M<sub>n</sub>*<sub>PS</sub> = 6100/7400 (by GPC).

**Figure 1.** <sup>13</sup>C NMR spectrum of C<sub>60</sub>-(PBOS)<sub>2</sub>-1 in CS<sub>2</sub>/(CD<sub>3</sub>)<sub>2</sub>-CO = 4:1.

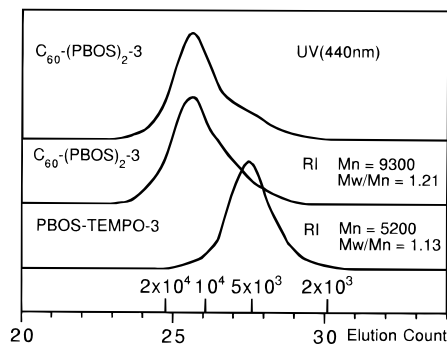
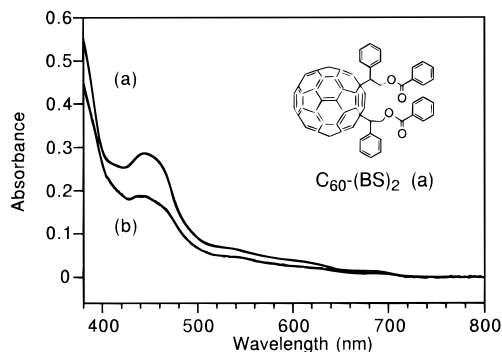
C<sub>60</sub> at a high temperature. The preparation and characterization of the PBOS-TEMPO and PS-PBOS-TEMPO adducts used in this work were described in detail elsewhere.<sup>10</sup> A possible mechanism by which the PS bisadducts are selectively produced was proposed previously,<sup>5</sup> which should also apply to the PBOS and PS-PBOS systems.

Table 1 summarizes the result of the reaction of the TEMPO adducts with C<sub>60</sub>. The yields (for definition, see footnote c to Table 1) of the purified products, which we designate as C<sub>60</sub>-(PBOS)<sub>2</sub> and C<sub>60</sub>-(PS-PBOS)<sub>2</sub>, ranged from 30% to 50%, showing no clear dependence on the molecular weight of the precursor alkoxyamine.

Figure 1 shows the <sup>13</sup>C NMR spectrum of C<sub>60</sub>-(PBOS)<sub>2</sub>-1, where the attached number shows the code number of the precursor alkoxyamine. In addition to the peaks derived from the PBOS moiety, the aromatic carbons derived from the C<sub>60</sub> moiety and the ipso carbon in the BOS unit attached to C<sub>60</sub> are observed between 140 and 160 ppm.

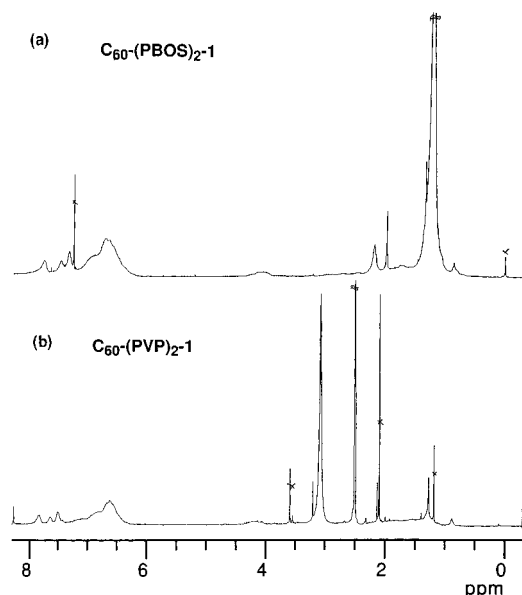
Figure 2 shows the GPC curves of C<sub>60</sub>-(PBOS)<sub>2</sub>-3 recorded by different detectors. The PBOS moiety is detectable by both UV-270 nm and RI, but not by UV-440 nm, while the C<sub>60</sub> moiety is detectable by all UV-440 nm, UV-270 nm, and RI. The two GPC curves of C<sub>60</sub>-(PBOS)<sub>2</sub>-3 are nearly identical with each other, which indicates a chemical uniformity of the polymer. The two curves retain a narrow polydispersity and commonly show an *M<sub>n</sub>* value of 9300, which is about twice that of the precursor PBOS-TEMPO-3. Similar results were obtained for all other samples (Table 1). This indicates that the reaction of PBOS-TEMPO with C<sub>60</sub> leads predominantly to a bisadduct, as in the case of PS-TEMPO.

Figure 3 compares the UV-vis spectra from C<sub>60</sub>-(BS)<sub>2</sub> and C<sub>60</sub>-(PBOS)<sub>2</sub>-1 solutions, where BS is the

**Figure 2.** GPC curves for C<sub>60</sub>-(PBOS)<sub>2</sub>-3 by UV (440 nm) and RI compared with that for PBOS-TEMPO-3 by RI.**Figure 3.** UV-vis spectra of (a) C<sub>60</sub>-(BS)<sub>2</sub> and (b) C<sub>60</sub>-(PBOS)<sub>2</sub>-1 in cyclohexane ( $6.63 \times 10^{-2}$  g mL<sup>-1</sup>).

[2-(benzoyloxy)-1-phenyl]ethyl group.<sup>5</sup> The two spectra are very similar to each other. This means that the polymer derivative is also a 1,4-bisadduct, like C<sub>60</sub>-(BS)<sub>2</sub> and C<sub>60</sub>-(PS)<sub>2</sub>.<sup>5</sup> On the basis of the molar absorption coefficient of C<sub>60</sub>-(BS)<sub>2</sub> at 440 nm, the *M<sub>n</sub>* of the polymer derivatives was estimated (Table 1). Generally, the values of *M<sub>n</sub>* by GPC and those by UV well agree with each other, and both are close to those calculated for the bisadduct structure. (The GPC value for the lowest molecular weight sample C<sub>60</sub>-(PBOS)<sub>2</sub>-1 is appreciably smaller than the UV and calculated values. This is ascribed to the C<sub>60</sub> moiety contributing little to the hydrodynamic volume of the molecule. As the molecular weight of the PBOS moiety increases, this effect becomes less important.<sup>5</sup>) We thus conclude that the reaction of PBOS-TEMPO or PBOS-PS-TEMPO with C<sub>60</sub> provides well-defined PBOS- or PBOS-PS-disubstituted 1,4-dihydro[60]fullerenes, selectively.

**Hydrolysis of C<sub>60</sub>-(PBOS)<sub>2</sub> and C<sub>60</sub>-(PS-PBOS)<sub>2</sub>.** The hydrolysis of the BOS units of the above-mentioned C<sub>60</sub> derivatives gave PVP polymers of the types C<sub>60</sub>-(PVP)<sub>2</sub> and C<sub>60</sub>-(PS-PVP)<sub>2</sub> (see the Experimental Section.) The <sup>1</sup>H NMR spectrum of C<sub>60</sub>-(PVP)<sub>2</sub>-1 is shown in Figure 4. The peak at 1.3 ppm ascribed to the *tert*-



**Figure 4.**  $^1\text{H}$  NMR spectra of (a)  $\text{C}_{60}\text{-(PBOS)}_{2-1}$  in  $\text{CS}_2/(\text{CD}_3)_2\text{-CO} = 4:1$  and (b)  $\text{C}_{60}\text{-(PVP)}_{2-1}$  in DMSO.

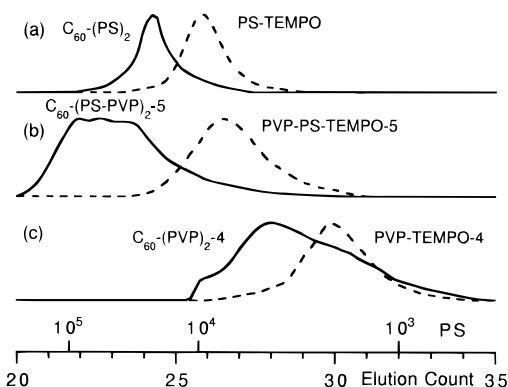


**Figure 5.** GPC curves of (a)  $\text{C}_{60}\text{-(PS)}_2$  ( $M_n = 10\,000$ ,  $M_w/M_n = 1.14$ ), (b)  $\text{C}_{60}\text{-(PS-PVP)}_{2-5}$ , and (c)  $\text{C}_{60}\text{-(PVP)}_{2-4}$  in THF by RI detector. The broken lines are for the respective precursor TEMPO adducts.

butyl group in BOS disappeared and the hydroxyl proton peak at 3.1 ppm newly appeared, which suggests a complete hydrolysis of the BOS unit. This was confirmed also by a  $^{13}\text{C}$  NMR analysis.

**Solute Dispersion State Viewed by GPC.** Figure 5 compares the GPC curves of  $\text{C}_{60}\text{-(PS)}_2$  ( $M_n = 10\,000$ ,  $M_w/M_n = 1.14$ ),<sup>5</sup>  $\text{C}_{60}\text{-(PVP)}_{2-4}$ , and  $\text{C}_{60}\text{-(PS-PVP)}_{2-5}$  along with those of their precursor alkoxyamines. All these  $\text{C}_{60}$  derivatives (as well as their precursors) have nearly the same molecular weight and a low polydispersity ( $M_w/M_n \leq 1.15$ ), according to the PS-calibrated GPC study made in THF before removing the *tert*-butyl groups. This hydrolysis is unlikely to cause degradation of the main chain. Nevertheless, the GPC curves of the PVP-containing polymers are very different from those of the PS polymers in two main aspects, as Figure 5 shows. First, the elution time of PVP-TEMPO-4 is appreciably longer, and its elution profile is somewhat broader, than those of the PS-TEMPO counterpart. This suggests that PVP is less soluble and has a smaller hydrodynamic volume in THF than PS and/or that there is some attractive mean force between PVP and the stationary phase. This effect is still observable, though less markedly, for PVP-PS-TEMPO-5. Second and more notably, the elution curves for the PVP-containing

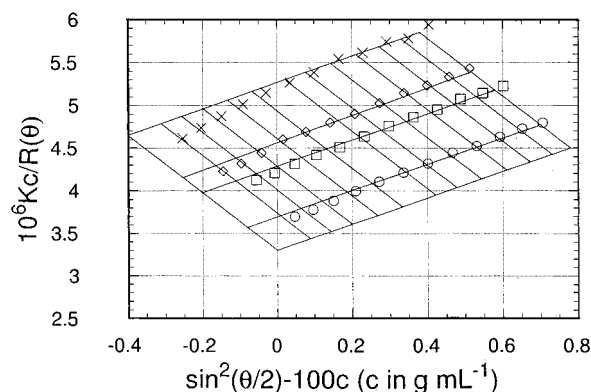


**Figure 6.** Zimm plot for  $\text{C}_{60}\text{-(PVP)}_{2-4}$  in THF at  $25.0\text{ }^\circ\text{C}$ .

**Table 2.** Values of  $M_w$  of  $\text{C}_{60}$  Experimentally Observed in THF at  $25\text{ }^\circ\text{C}$  and Those Calculated

| code                                  | $10^{-5}M_{w,\text{exp}}$ | $10^{-4}M_{w,\text{calcd}}$ | $M_{w,\text{exp}}/M_{w,\text{calcd}}$ |
|---------------------------------------|---------------------------|-----------------------------|---------------------------------------|
| $\text{C}_{60}\text{-(PVP)}_{2-4}$    | 3.0 <sup>a</sup>          | 1.4 <sup>c</sup>            | 21                                    |
| $\text{C}_{60}\text{-(PS-PVP)}_{2-5}$ | 1.5 <sup>b</sup>          | 2.4 <sup>d</sup>            | 6.3                                   |

<sup>a</sup> Determined by light scattering with  $dn/dc = 0.138\text{ mL/g}$ . <sup>b</sup> Determined by light scattering with  $dn/dc = 0.172\text{ mL/g}$ . <sup>c</sup> Calculated for the bisadduct structure using the GPC value for PBOS-TEMPO-4 (Table 1). <sup>d</sup> Calculated for the bisadduct structure using the GPC value for PBOS-PS-TEMPO-5 (Table 1).

$\text{C}_{60}$  derivatives are composed of multiple peaks and strangely skewed, indicating the formation of multimolecular micelles of various sizes. Judging from the GPC curves, the micelle size of  $\text{C}_{60}\text{-(PS-PVP)}_{2-5}$  may appear to be larger than that of  $\text{C}_{60}\text{-(PVP)}_{2-4}$ . However, this cannot be concluded since the micellar size is generally a function of concentration, and the concentration of the solutes migrating through the GPC column is not uniquely defined. Moreover, the possible solute-gel interaction suggested above would make it difficult to judge micellar sizes by GPC profiles. In fact, light scattering shows that  $\text{C}_{60}\text{-(PVP)}_{2-4}$  forms a larger micelle in THF than the other derivative does (see below).

**Micellization Behavior Studied by Light Scattering.** Static light-scattering measurements were made for the THF solutions of  $\text{C}_{60}\text{-(PVP)}_{2-4}$  and  $\text{C}_{60}\text{-(PS-PVP)}_{2-5}$ . To obtain an idea about the sizes of the micelles possibly formed by these polymers, the scattered light intensities ( $I$ ) from their solutions with a fixed concentration (0.5 wt %) were measured at a fixed angle ( $90^\circ$ ) and compared with the intensities from the solutions of their precursors PVP-TEMPO-4 and PVP-PS-TEMPO-5, respectively, measured under the same conditions. The intensity ratios were found to be  $I[\text{C}_{60}\text{-(PVP)}_{2-4}]/I[\text{PVP-TEMPO-4}] = 15$  and  $I[\text{C}_{60}\text{-(PS-PVP)}_{2-5}]/I[\text{PVP-PS-TEMPO-5}] = 6$  respectively. This indicates that micelles formed by several molecules of the  $\text{C}_{60}$ -polymer exist in the THF solution in both cases, since the precursors can be assumed to be molecularly dispersed in THF.

To obtain more quantitative information, light-scattering measurements were made for the  $\text{C}_{60}$ -polymers at varying angles and concentrations. An example of the Zimm diagram is given in Figure 6. The obtained values of  $M_w$  are compared with the theoretical (unimolecular) values in Table 2. Clearly, the  $\text{C}_{60}$ -polymers form in THF micelles composed of about 21 and 6 molecules of  $\text{C}_{60}\text{-(PVP)}_{2-4}$  and  $\text{C}_{60}\text{-(PS-PVP)}_{2-5}$ , respectively. Namely, the association number of the  $\text{C}_{60}$ -polymer with the homo-PVP arms is larger than

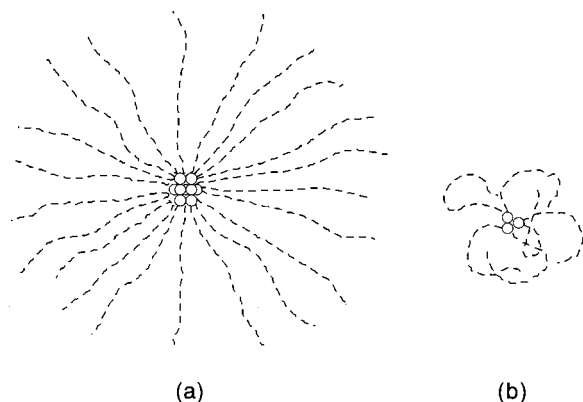


**Figure 7.** Schematic representation of multimolecular micelles formed by (a)  $C_{60}$ -(PVP)<sub>2</sub>-4 and (b)  $C_{60}$ -(PS-PVP)<sub>2</sub>-5 in THF at 25 °C.

that with the PS-PVP block-copolymer arms. The derivatives of the type  $C_{60}$ -(PS)<sub>2</sub> are molecularly dispersed in THF, according to the previous GPC study.<sup>5</sup> Recalling that THF is a better solvent for PS than for PVP and that it will give an intermediate solubility to PVP-PS block copolymers, we may tentatively suggest that the poorer is the solvent toward the polymer moiety, the stronger is the association tendency of  $C_{60}$ -polymer,<sup>5</sup> if compared at a common level of molecular weight. Since the  $C_{60}$  moiety is hardly soluble in THF, the micelles formed by a  $C_{60}$ -polymer will have a core of the  $C_{60}$  moieties surrounded by the fringes of the polymer moieties, as illustrated in Figure 7. Such a core-fringes structure is somewhat similar to the one often observed for block-copolymer micelles formed in dilute solution with a selective solvent.<sup>12,13</sup>

It is also noted that the Zimm plot in Figure 6 seems quite normal, giving no indication of increasing association number with increasing concentration nor suggesting micelle dissociation at low concentrations. The straight concentration envelope with a positive slope (positive apparent second virial coefficient) implies that the micelles are stable in the studied range of concentration,  $1 < 10^3 C \text{ (g/mL)} < 4$ . In a strict sense, the light-scattering values of  $M_w$  given above are apparent ones, since the  $C_{60}$ -polymers, particularly  $C_{60}$ -(PS-PVP)<sub>2</sub>-5, are not uniform in the refractive index increment ( $dn/dc$ ) along the chain, so that any distribution in the chain lengths of the PS and/or PVP moieties brings about a distribution of composition (hence  $dn/dc$ ) among different molecules. This invalidates the simple light-scattering theory.<sup>14</sup> The effect of composition heterogeneity, however, should be rather minor in the present systems, since the polymers are fairly narrow in chain length distribution. Moreover, multimolecular micellization will effectively average out the composition heterogeneity, if there is any.<sup>12a</sup> The slope of the angular envelope in Figure 6 suggests a micelle radius of gyration,  $R_g$ , on the order of 40 nm. This value appears to be somewhat too large for the micellar structure suggested in Figure 7 and may not be very reliable. A possible cause for the overestimation of  $R_g$  may be the difficulty in preparing perfectly dust-free solutions (because of the limited amount of the  $C_{60}$ -polymer available). Nevertheless, the comparison of this  $R_g$  with the value of about 20 nm obtained for the  $C_{60}$ -(PS-PVP)<sub>2</sub>-5 solutions, which were purified similarly, suggests that the polymer fringes in the  $C_{60}$ -(PVP)<sub>2</sub>-4 micelles are appreciably more extended than those in the  $C_{60}$ -(PS-

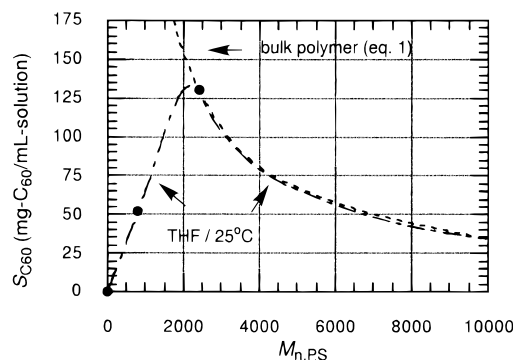


**Figure 8.** Saturation solubility  $S_{C_{60}}$  of the  $C_{60}$  moiety in THF at 25 °C as a function of the  $M_n$  of the PS arm (dot-dash line). The dotted line shows eq 1.

PVP)<sub>2</sub>-5 micelles because of a higher steric hindrance in the former than in the latter, as illustrated in Figure 7.

**Saturation Solubilities of  $C_{60}$ -(PS)<sub>2</sub> and  $C_{60}$ -(PVP)<sub>2</sub>.** As already noted, THF is a good solvent for PS and a nonsolvent for  $C_{60}$ . Thus it is expected that a  $C_{60}$ -(PS)<sub>2</sub> adduct with PS chains shorter than a critical length will have a limited solubility in THF depending on the PS chain length. Adducts with PS chains longer than the critical length will be miscible with THF in all proportions. In fact, the adduct with a molecular weight of the PS chain,  $M_{n,PS}$ , of about 1000 showed a limited miscibility with THF, the saturation solubility being 190 mg/mL of solution. On the other hand, the adduct with  $M_{n,PS} \approx 2400$  seems to be soluble in THF at all concentrations.

In view of the generally poor solubility of  $C_{60}$  in solvents and polymers, more interesting is the saturation solubility  $S_{C_{60}}$  of the  $C_{60}$  moiety rather than that of the adduct as a whole. When the chain length of the PS moiety increases, the concentration of the  $C_{60}$  moiety within the bulk adduct decreases according to

$$S_{C_{60}} = (M_{C_{60}}/M_{\text{adduct}})d_{\text{adduct}} \quad (1)$$

Here,  $M_{C_{60}}$  and  $M_{\text{adduct}}$  are the (number-average) molecular weights of the  $C_{60}$  moiety and the whole adduct, respectively, and  $d_{\text{adduct}}$  is the adduct density, which we approximate here by the PS density of 1.06 g/mL. Equation 1 is shown by the dotted line in Figure 8, and it gives the maximum possible values of  $S_{C_{60}}$  in any solvent. When a  $C_{60}$ -polymer adduct shows a limited solubility in a given solvent, its value of  $S_{C_{60}}$  is necessarily smaller than the dotted line. Therefore, the  $S_{C_{60}}$  of the  $C_{60}$ -(PS)<sub>2</sub>/THF system should behave like the dot-dash line in Figure 8, which is schematic to some extent because of the lack of a sufficient number of data points.

All the  $C_{60}$ -(PVP)<sub>2</sub> samples prepared in this work showed a limited solubility in THF. Figure 9 gives  $S_{C_{60}}$  as a function of the molecular weight of the PVP chain,  $M_{n,PVP}$ .  $S_{C_{60}}$  is considerably smaller than the maximum possible value for the bulk adduct and seems to have a peak at around  $M_{n,PVP} = 1000$ , where about 16 mg of the  $C_{60}$  moiety can be solubilized in 1 mL of THF solution. This maximum value of  $S_{C_{60}}$  is considerably smaller than the one attainable by the PS adduct (Figure 8). This is ascribed to the poorer solubility of PVP in THF than that of PS and is consistent with the micellization tendency described in previous sections.

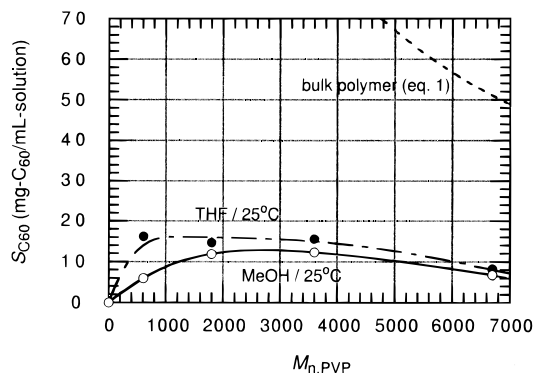


**Figure 9.** Saturation solubility  $S_{C_{60}}$  of the  $C_{60}$  moiety in THF (dot-dash line) and in methanol (solid line) at 25 °C as a function of the  $M_{n,PVP}$  of the attached PVP chain.

In this connection, it should be remembered that both the GPC and light scattering studies on the micellization behavior were made at very low concentrations. For example, the highest concentration of  $C_{60}$ -(PVP)<sub>2</sub>-4 studied by light scattering (Figure 6) is 4.0 mg/mL in the adduct concentration or about 0.04 mg/mL in the  $C_{60}$ -moiety concentration, which, of course, is far below the saturation-solubility line in Figure 9. Since micelles formed at low concentrations are unlikely to dissociate to single molecules at higher concentrations, it is indicated that  $C_{60}$ -(PVP)<sub>2</sub> adducts are solubilized in THF in a multimolecular micellar form in virtually the whole region below the  $S_{C_{60}}$  line. On the other hand, all available  $C_{60}$ -(PS)<sub>2</sub> adducts ( $M_{n,PS} \geq 1000$ ) are molecularly dispersed in dilute THF solution, as is judged from their GPC curves.<sup>5</sup> It is an interesting open question whether they remain in a molecularly dispersed state when the concentration is increased toward the  $S_{C_{60}}$  line in Figure 8. This question is somehow related to the likewise interesting and important one as to the molecular dispersion state in bulk  $C_{60}$ -polymers.

Another interesting topic is the solubility of  $C_{60}$ -(PVP)<sub>2</sub> adducts in polar solvents. We have determined the saturation solubilities of the PVP adducts in methanol, which seemingly is a good solvent for PVP. As in THF, however, all the  $C_{60}$ -(PVP)<sub>2</sub> adducts showed a limited solubility in methanol. Figure 9 gives  $S_{C_{60}}$  as a function of  $M_{n,PVP}$ . This  $S_{C_{60}}$  curve is similar in shape and magnitude to that in THF and suggests that methanol is not a strong enough solvent to disperse the adduct monomolecularly; namely, it is highly likely that the molecules are dissolved in methanol, forming multimolecular micelles again. At this time, it is not possible to confirm this by light scattering due to the technical difficulty of conducting measurements in methanol. In any case, it should be stressed that the  $C_{60}$  moiety can be made soluble in the polar solvent in concentrations over 1 wt % by the PVP derivatization.

**Micellization Behavior Studied by UV-Vis Spectra.** The electronic properties of  $C_{60}$  are affected by its environment. Estoe<sup>8a</sup> reported that the UV-vis spectrum of the  $C_{60}$  molecules solubilized in water in a colloidal form by use of a surfactant is markedly different from that of the molecules in a monomeric dispersion state. Figure 10 shows the UV-vis spectra of three derivatives of nearly the same size (in THF):  $C_{60}$ -(PS)<sub>2</sub> (solid line;  $M_{n,PS} = 5500$ ,  $M_w/M_n = 1.18$ ),  $C_{60}$ -(PS-PVP)<sub>2</sub>-5 (broken line), and  $C_{60}$ -(PVP)<sub>2</sub>-4 (dotted line).  $C_{60}$ -(PS)<sub>2</sub> shows the spectrum characteristic of

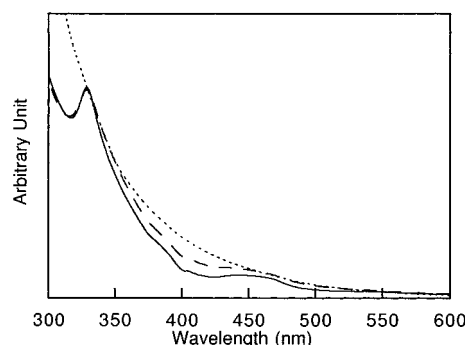


**Figure 10.** UV-vis spectra of  $C_{60}$ -(PS)<sub>2</sub> (solid line;  $M_n = 5500$ ,  $M_w/M_n = 1.18$ ),  $C_{60}$ -(PS-PVP)<sub>2</sub>-5 (broken line), and  $C_{60}$ -(PVP)<sub>2</sub>-4 (dotted line) in THF.

1,4-disubstituted  $C_{60}$ , while  $C_{60}$ -(PVP)<sub>2</sub> gives a spectrum with no absorption maxima, which is rather similar to the one observed for the pure  $C_{60}$  in water in a colloidal form.<sup>8a</sup> On the other hand, the 440 nm peak of  $C_{60}$ -(PS-PVP)<sub>2</sub> is somewhat broadened and appears between the spectra of  $C_{60}$ -(PS)<sub>2</sub> and  $C_{60}$ -(PVP)<sub>2</sub>. Remembering that the association numbers of the PVP, PS-PVP, and PS derivatives observed in this solvent are 21, 6, and 1 (no association), respectively, and that the colloidal micelles of  $C_{60}$  observed in water are of a macroscopic size, we may conclude that UV-vis spectroscopy offers a quick and convenient means to study the dispersion state of  $C_{60}$  compounds. It can even inform us of the approximate micellar size, if the association number is not too large, e.g., <10–20.

## Conclusions

Low-polydispersity 1,4-disubstituted  $C_{60}$  derivatives of the types  $C_{60}$ -(PVP)<sub>2</sub> and  $C_{60}$ -(PS-PVP)<sub>2</sub> were prepared by applying the nitroxide-controlled free radical polymerization technique and studied along with their solubility behaviors in comparison with those of the  $C_{60}$ -(PS)<sub>2</sub> adducts prepared previously by the similar procedure.<sup>5</sup>

Both GPC and light-scattering studies showed that  $C_{60}$ -(PVP)<sub>2</sub> and  $C_{60}$ -(PS-PVP)<sub>2</sub> form multimolecular micelles in THF at 25 °C. More specifically, the light-scattering study showed that  $C_{60}$ -(PVP)<sub>2</sub> and  $C_{60}$ -(PS-PVP)<sub>2</sub> with  $M_n$  roughly about  $10^4$  form stable micelles in dilute solution ( $10^{-3} < C < 10^{-2}$  g/mL) with association numbers of about 20 and 6, respectively. On the other hand,  $C_{60}$ -(PS)<sub>2</sub> showed no indication of association in this solvent at least in dilute solution.

Except for the sample with the shortest (available) PS chain ( $M_{n,PS} \approx 1000$ ),  $C_{60}$ -(PS)<sub>2</sub> seemed miscible with THF in all proportions, while all the available  $C_{60}$ -(PVP)<sub>2</sub> samples ( $M_{n,PVP} < 10\,000$ ) showed a limited solubility in THF. Thus the solvent power toward the polymer moiety in a  $C_{60}$ -polymer adduct is reflected on both the saturation solubility and the micellization behavior in a consistent manner.

The maximum solubility of the  $C_{60}$  moiety in THF was found to exceed 100 mg/mL with  $C_{60}$ -(PS)<sub>2</sub> and about 18 mg/mL with  $C_{60}$ -(PVP)<sub>2</sub>. The  $C_{60}$  moiety in  $C_{60}$ -(PVP)<sub>2</sub> can be made soluble even in a polar solvent (methanol) as much as 18 mg/mL. These maximum solubilities of the  $C_{60}$  moiety are commonly achieved with a polymer chain length in the range 1000–3000 in  $M_n$ .

The 440 nm absorption peak can be used as a measure of the dispersion state and micellar size of  $C_{60}$  derivatives in solution.

The experimental data given in this paper were limited to those C<sub>60</sub>-polymers with relatively low molecular weights. With an increase in the molecular weight of the polymer moiety, the solubility behaviors of the C<sub>60</sub>-polymers should approach to those of the polymer moieties, with the effects of the C<sub>60</sub> moiety becoming less and less important. In this context, the conclusions given in this work can be regarded as general.

**Acknowledgment.** This work was supported by a Grant-in-Aid for Scientific Research, the Ministry of Education, Science, Sports, and Culture, Japan (Grant-in-Aid 09450351 and 09238226).

## References and Notes

- (1) (a) Kroto, H. W.; Allaf, A. W.; Balm, S. P. *Chem. Rev.* **1991**, *91*, 1213. (b) Wudl, F. *Acc. Chem. Res.* **1992**, *25*, 157. (c) Talor, R.; Walton, D. R. M. *Nature* **1993**, *363*, 685. Olah, G. A.; Bucsi, I.; Aniszfeld, R.; prakash, G. K. S. *Carbon* **1992**, *30*, 1203. (d) Hirsch, A. *The Chemistry of the Fullerenes*; Georg Thieme Verlag: Stuttgart, 1994. (e) Boyd, P. D. W.; Bhayrapa, P.; Paul, P.; Stinchcombe, J.; Bolskar, R. D.; Sun, Y.-P.; Reed, C. A. *J. Am. Chem. Soc.* **1995**, *117*, 2907. See also: (f) Diederich, F.; Thilgen, C. *Science* **1996**, *271*, 317 and references therein.
- (2) Okamura, H.; Minoda, M.; Komatsu, K.; Miyamoto, T. *Macromol. Chem. Phys.* **1997**, *198*, 777.
- (3) Weis, C.; Friedrich, C.; Mulhaupt, R.; Frey, H. *Macromolecules* **1995**, *28*, 403.
- (4) (a) Sun, Y.-P.; Ma, B.; Bunker, C. E.; Liu, B. *J. Am. Chem. Soc.* **1995**, *117*, 12705. (b) Loy, D. A.; Roger, A. A. *J. Am. Chem. Soc.* **1992**, *114*, 3977. (c) Shi, K.; Khemani, K. C.; Li, Q.; Wudl, F. *J. Am. Chem. Soc.* **1992**, *114*, 10656. (d) Hawker, C. J. *Macromolecules* **1994**, *27*, 4836. (e) Benincori, T.; Brenna, E.; Sanniccolo, F.; Trimarco, L.; Zotti, G.; Sozzani, P. *Angew. Chem., Int. Ed. Engl.* **1996**, *35*, 648. (f) Chiang, L. Y.; Wang, L. Y.; Kuo, C. S. *Macromolecules* **1995**, *28*, 7574. (g) Samulski, E. T.; DeSimone, J. W.; Hunt, M. G., Jr.; Mencelogu, Y. Z.; Jarhagin, R. C.; York, G. A.; Labet, K. B.; Wang, H. *Chem. Mater.* **1992**, *4*, 9665. (h) Weis, C.; Friedrich, C.; Mulhaupt, R.; Frey, H. *Macromolecules* **1995**, *28*, 403. (i) Hawker, C. J.; Wooley, K. L.; Frechet, J. M. *J. Chem. Soc., Chem. Commun.* **1994**, 925. (j) Wignall, G. D.; Affholter, K. A.; Bunick, G. J.; Hunt, M. O., Jr.; Mencelogu, Y. Z.; DeSimone, J. M.; Samulski, E. T. *Macromolecules* **1995**, *28*, 6000. (k) Weis, C.; Friedrich, C.; Mulhaupt, R.; Frey, H. *Macromolecules* **1995**, *28*, 403. (l) Cao, T.; Webber, S. E. *Macromolecules* **1995**, *28*, 3741. (m) Bunker, C. E.; Lawson, G. E.; Sun, Y.-P. *Macromolecules* **1995**, *28*, 3744. (n) Sun, Y.-P.; Lawson, G. E.; Bunker, C. E.; Johnson, R. A.; Ma, B.; Farmer, C.; Riggs, J. E.; Kitaygorodskiy, A. *Macromolecules* **1996**, *29*, 8441. (o) Camp, A. G.; Lary, A.; Ford, W. T. *Macromolecules* **1995**, *28*, 7959. (p) Sun, Y.-P.; Liu, B.; Moton, D. K. *Chem. Commun.* **1996**, 2699.
- (5) Okamura, H.; Terauchi, T.; Minoda, M.; Fukuda, T.; Komatsu, K. *Macromolecules* **1997**, *30*, 5279.
- (6) Ederle, Y.; Mathis, C. *Macromolecules* **1997**, *30*, 2546. Ederle, Y.; Mathis, C. *Fullerene Sci. Technol.* **1996**, *4*, 1177.
- (7) Ruoff, R. S.; Tse, D. S.; Malhorta, R.; Lorents, D. C. *J. Phys. Chem.* **1993**, *97*, 3379.
- (8) (a) Eastoe, J.; Crooks, E. R.; Beeby, A.; Heenan, R. K. *Chem. Phys. Lett.* **1995**, *245*, 571. (b) Matsumoto, M.; Tachibana, H.; Azumi, R.; Tanaka, M.; Nakamura, T.; Yunome, G.; Abe, M.; Yamago, S.; Nakamura, E. *Langmuir* **1995**, *11*, 660. (c) Diederich, F.; Effing, J.; Jonas, U.; Jullien, L.; Plesnivy, T.; Ringsdorf, H.; Thilgen, C.; Weistein, D. *Angew. Chem., Int. Ed. Engl.* **1992**, *31*, 1599.
- (9) (a) Solomon, D. H.; Rizzardo, E.; Cacioli, P. U.S. Patent 4, 581, 429. (b) Rizzardo, E. *Chem. Aus.* **1987**, *54*, 32. (c) Georges, M. K.; Veregin, R. P. N.; Kazmaier, P. M.; Hamer, G. K. *Macromolecules* **1993**, *26*, 2987. (d) Fukuda, T.; Terauchi, T.; Goto, A.; Ohno, K.; Tsujii, Y.; Miyamoto, T.; Kobatake, S.; Yamada, B. *Macromolecules* **1996**, *29*, 6393. (e) Fukuda, T.; Goto, A.; Ohno, K.; Tsujii, Y. In *Advances in Free Radical Polymerization*; Matyjaszewski, K., Ed.; ACS Symposium Series; American Chemical Society: Washington, DC, (in press).
- (10) Ohno, K.; Ejaz, M.; Fukuda, T.; Miyamoto, T. *Macromol. Chem. Phys.*, in press.
- (11) Higashimura, T.; Kojima, K.; Sawamoto, M. *Makromol. Chem., Suppl.* **1989**, *15*, 127.
- (12) (a) Kotaka, T.; Tanaka, T.; Hattori, M.; Inagaki, H. *Macromolecules* **1978**, *11*, 138. (b) Tanaka, T.; Kotaka, T.; Inagaki, H. *Polym. J.* **1972**, *3*, 338.
- (13) Kraus, S. *J. Phys. Chem.* **1964**, *68*, 1948.
- (14) Bushok, W.; Benoit, H. *Can. J. Chem.* **1958**, *36*, 1616.

MA971696S